

2018-04-10

A Strong Limit on the Very-high-energy Emission from GRB 150323A

P. T. Reynolds

Department of Physical Sciences, Cork Institute of Technology, Bishopstown, Cork, Ireland

et al

Follow this and additional works at: <https://sword.cit.ie/dptphysciart>



Part of the [External Galaxies Commons](#), and the [Stars, Interstellar Medium and the Galaxy Commons](#)

Recommended Citation

Abeysekara, A.U., Archer, A., Benbow, W., Bird, R., Brose, R., Buchovecky, M., Bugaev, V., Connolly, M.P., Cui, W., Errando, M., Falcone, A., Feng, Q., Finley, J.P., Flinders, A., Fortson, L., Furniss, A., Gillanders, G.H., Hütten, M., Hanna, D., Hervet, O., Holder, J., Hughes, G., Humensky, T.B., Johnson, C.A., Kaaret, P., Kar, P., Kelley-Hoskins, N., Kertzman, M., Kieda, D., Krause, M., Krennrich, F., Lang, M.J., Lin, T.T.Y., Maier, G., McArthur, S., Moriarty, P., Mukherjee, R., O'Brien, S., Ong, R.A., Park, N., Perkins, J.S., Petrashyk, A., Pohl, M., Popkow, A., Poeschel, E., Quinn, J., Ragan, K., Reynolds, P.T., Richards, G.T., Roache, E., Rulten, C., Sadeh, I., Santander, M., Sembroski, G.H., Shahinyan, K., Tyler, J., Wakely, S.P., Weiner, O.M., Weinstein, A., Wells, R.M., Wilcox, P., Wilhelm, A., Williams, D.A., Zitzer, B., Vurm, I. and Beloborodov, A. (2018). A Strong Limit on the Very-high-energy Emission from GRB 150323A. *The Astrophysical Journal*, [online] 857(1), p.33. Available at: <https://iopscience.iop.org/article/10.3847/1538-4357/aab371>

This Article is brought to you for free and open access by the Physical Sciences at SWORD - South West Open Research Deposit. It has been accepted for inclusion in Physical Sciences Publications by an authorized administrator of SWORD - South West Open Research Deposit. For more information, please contact sword@cit.ie.



A Strong Limit on the Very-high-energy Emission from GRB 150323A

A. U. Abeysekara¹, A. Archer², W. Benbow³ , R. Bird⁴ , R. Brose^{5,6}, M. Buchovecky⁴, V. Bugaev², M. P. Connolly⁷, W. Cui^{8,9} , M. Errando² , A. Falcone¹⁰, Q. Feng¹¹ , J. P. Finley⁸ , A. Flinders¹, L. Fortson¹², A. Furniss¹³ , G. H. Gillanders⁷ , M. Hütten⁶, D. Hanna¹¹ , O. Hervet¹⁴, J. Holder¹⁵, G. Hughes³, T. B. Humensky¹⁶, C. A. Johnson¹⁴ , P. Kaaret¹⁷ , P. Kar¹, N. Kelley-Hoskins⁶, M. Kertzman¹⁸, D. Kieda¹ , M. Krause⁶ , F. Krennrich¹⁹, M. J. Lang⁷ , T. T. Y. Lin¹¹, G. Maier⁶ , S. McArthur⁸, P. Moriarty⁷, R. Mukherjee²⁰ , S. O'Brien²¹, R. A. Ong⁴, N. Park²², J. S. Perkins²³ , A. Petraschuk¹⁶, M. Pohl^{5,6} , A. Popkow⁴ , E. Pueschel⁶ , J. Quinn²¹, K. Ragan¹¹, P. T. Reynolds²⁴, G. T. Richards²⁵ , E. Roache³, C. Rulten¹², I. Sadeh⁶, M. Santander²⁰, G. H. Sembroski⁸, K. Shahinyan¹² , J. Tyler¹¹, S. P. Wakely²², O. M. Weiner¹⁶, A. Weinstein¹⁹, R. M. Wells¹⁹, P. Wilcox¹⁷, A. Wilhelm^{5,6}, D. A. Williams¹⁴ , B. Zitzer¹¹,

(VERITAS Collaboration)

Indrek Vurm¹⁶ , and Andrei Beloborodov¹⁶¹ Department of Physics and Astronomy, University of Utah, Salt Lake City, UT 84112, USA² Department of Physics, Washington University, St. Louis, MO 63130, USA³ Fred Lawrence Whipple Observatory, Harvard-Smithsonian Center for Astrophysics, Amado, AZ 85645, USA⁴ Department of Physics and Astronomy, University of California, Los Angeles, CA 90095, USA⁵ Institute of Physics and Astronomy, University of Potsdam, D-14476 Potsdam-Golm, Germany⁶ DESY, Platanenallee 6, D-15738 Zeuthen, Germany⁷ School of Physics, National University of Ireland Galway, University Road, Galway, Ireland⁸ Department of Physics and Astronomy, Purdue University, West Lafayette, IN 47907, USA⁹ Department of Physics and Center for Astrophysics, Tsinghua University, Beijing 100084, People's Republic of China¹⁰ Department of Astronomy and Astrophysics, 525 Davey Lab, Pennsylvania State University, University Park, PA 16802, USA¹¹ Physics Department, McGill University, Montreal, QC H3A 2T8, Canada¹² School of Physics and Astronomy, University of Minnesota, Minneapolis, MN 55455, USA¹³ Department of Physics, California State University - East Bay, Hayward, CA 94542, USA¹⁴ Santa Cruz Institute for Particle Physics and Department of Physics, University of California, Santa Cruz, CA 95064, USA¹⁵ Department of Physics and Astronomy and the Bartol Research Institute, University of Delaware, Newark, DE 19716, USA¹⁶ Physics Department, Columbia University, New York, NY 10027, USA; omw2107@columbia.edu, indrek.vurm@gmail.com¹⁷ Department of Physics and Astronomy, University of Iowa, Van Allen Hall, Iowa City, IA 52242, USA¹⁸ Department of Physics and Astronomy, DePauw University, Greencastle, IN 46135-0037, USA¹⁹ Department of Physics and Astronomy, Iowa State University, Ames, IA 50011, USA²⁰ Department of Physics and Astronomy, Barnard College, Columbia University, NY 10027, USA; rmukherj@barnard.edu²¹ School of Physics, University College Dublin, Belfield, Dublin 4, Ireland²² Enrico Fermi Institute, University of Chicago, Chicago, IL 60637, USA²³ N.A.S.A./Goddard Space-Flight Center, Code 661, Greenbelt, MD 20771, USA²⁴ Department of Physical Sciences, Cork Institute of Technology, Bishopstown, Cork, Ireland²⁵ School of Physics and Center for Relativistic Astrophysics, Georgia Institute of Technology, 837 State Street NW, Atlanta, GA 30332-0430, USA

Received 2017 August 16; revised 2018 January 26; accepted 2018 February 24; published 2018 April 10

Abstract

On 2015 March 23, the Very Energetic Radiation Imaging Telescope Array System (VERITAS) responded to a *Swift*-Burst Alert Telescope (BAT) detection of a gamma-ray burst, with observations beginning 270 s after the onset of BAT emission, and only 135 s after the main BAT emission peak. No statistically significant signal is detected above 140 GeV. The VERITAS upper limit on the fluence in a 40-minute integration corresponds to about 1% of the prompt fluence. Our limit is particularly significant because the very-high-energy (VHE) observation started only ~ 2 minutes after the prompt emission peaked, and *Fermi*-Large Area Telescope observations of numerous other bursts have revealed that the high-energy emission is typically delayed relative to the prompt radiation and lasts significantly longer. Also, the proximity of GRB 150323A ($z = 0.593$) limits the attenuation by the extragalactic background light to $\sim 50\%$ at 100–200 GeV. We conclude that GRB 150323A had an intrinsically very weak high-energy afterglow, or that the GeV spectrum had a turnover below ~ 100 GeV. If the GRB exploded into the stellar wind of a massive progenitor, the VHE non-detection constrains the wind density parameter to be $A \gtrsim 3 \times 10^{11} \text{ g cm}^{-1}$, consistent with a standard Wolf–Rayet progenitor. Alternatively, the VHE emission from the blast wave would be weak in a very tenuous medium such as the interstellar medium, which therefore cannot be ruled out as the environment of GRB 150323A.

Key words: gamma rays: general – gamma-ray burst: general – gamma-ray burst: individual (GRB 150323A)

1. Introduction

1.1. High-energy Radiation from Gamma-Ray Bursts

Gamma-ray bursts (GRBs) are thought to be powered by ultrarelativistic jets associated with the birth of a compact object. The bulk of their radiation is typically received over

several seconds (the so-called prompt emission), with spectral peaks clustering around a few hundred keV. In contrast, the more long-lived afterglows have been observed across the entire electromagnetic spectrum—from radio to GeV gamma-rays. In particular, the *Fermi*-Large Area Telescope (LAT) detects approximately 10 GRBs per year, or roughly 10% of

GRBs that occur in its field of view (Ackermann et al. 2013). The photon indices measured by LAT cluster around $\Gamma = 2$ (i.e., constant energy per logarithmic frequency interval), without a high-energy spectral break or cutoff; this suggests that substantial energy could be emitted above ~ 100 GeV, where it could be detected by imaging atmospheric Cherenkov telescopes (IACTs). LAT-detected afterglows roughly decay as $1/t$, with no clear cutoff and are often observed for hundreds of seconds before the emission becomes too faint for detection. In the case of the bright and nearby GRB 130427A, LAT detected the afterglow for several hours (Ackermann et al. 2014).

The main advantage of Cherenkov instruments is their large effective area, several orders of magnitude above space-based instruments such as LAT, which more than compensates for the smaller photon flux at very high energies (VHE; $E > 100$ GeV) unless the spectrum is extremely steep. Gamma-ray burst locations have indeed been observed by IACTs, and are considered a high-priority target. However, none have been detected to date (e.g., Albert et al. 2007; Aharonian et al. 2009; Acciari et al. 2011). Air-shower detectors, which are most sensitive at energies above ~ 10 TeV, have also failed to conclusively detect any of the bursts they observed (e.g., Abdo et al. 2007, Alfaro et al. 2017). There was a hint of possible emission from GRB 970417A; however, the significance of the signal was not considered high enough to indicate unambiguous detection (Atkins et al. 2000). Overall, these non-detections most likely imply a break in the high-energy spectrum in most GRBs.

The start of IACT observations is typically delayed by a few minutes relative to the prompt trigger, when the GRB has usually already entered the afterglow stage. In a sparse environment like the interstellar medium (ISM), such delays are comparable to the time it takes for the jet to transfer a sizable fraction of its kinetic energy to the external medium via the forward shock. Furthermore, given the typical jet Lorentz factors of a few hundred, the *average* energy available per particle at the shock is in the TeV range during the early afterglow. The external blast wave is thus expected to be a bright TeV emitter during the first minutes (e.g., Meszaros & Rees 1994), *regardless of the efficiency* of non-thermal particle acceleration at the shock. On the other hand, a lack of TeV emission from a bright nearby burst such as GRB 150323A may indicate that the jet has undergone rapid early deceleration in a dense environment such as the stellar wind of the Wolf-Rayet progenitor (Vurm & Beloborodov 2017). Thus, TeV emission constitutes a relatively clean probe of the GRB environment and early blast wave evolution.

1.2. VERITAS GRB Observations

VERITAS (the Very Energetic Radiation Imaging Telescope Array System) is an IACT array, which is the most sensitive type of instrument for detecting astrophysical gamma-ray emission at ~ 1 TeV energies (Holder et al. 2009). IACT arrays rely on the detection of Cherenkov light induced by particles in extensive air showers that were initiated by energetic astrophysical particles entering the atmosphere. The showers are imaged with multiple telescopes, allowing their incoming directions and energies to be reconstructed. VERITAS is sensitive to gamma-rays with energies from about 85 GeV to more than 30 TeV (Park 2005).

When VERITAS receives a burst alert through the GRB Coordinates Network (GCN; Barthelmy 2008), the on-site

observers are prompted to slew the telescopes to the burst position barring any constraints, such as the position of the Moon or the elevation of the burst. The delay between trigger and observation, which involves the arrival time of the alert, response by VERITAS observers, and telescope slewing, is usually on the order of a few minutes (Acciari et al. 2011).

GRBs have not been detected at energies greater than 100 GeV by any instrument to date. Previous observations of *Swift* GRBs by VERITAS placed limits on the possibility of particularly strong VHE emission from these bursts (Acciari et al. 2011). At the time of this work, VERITAS has observed more than 150 gamma-ray burst positions, with 50 observations made within 180 s of the satellite trigger time. Of these, follow-up observations exist for about 90 bursts detected by the *Swift*-Burst Alert Telescope (BAT), 90 bursts detected by *Fermi*-GBM, and 10 bursts detected by *Fermi*-LAT.

A study performed by Weiner (2015) attempted to isolate the most promising gamma-ray burst observations made by VERITAS. It only considered observations of bursts that have been well localized (compared to the VERITAS point-spread function) and for which a redshift has been measured. It took into account the most important factors (outside of the burst's VHE energy output, around which there can be much uncertainty) that impact the observability of a burst: redshift, observing elevation, and observing delay. Eight bursts were identified by this analysis, and none were detected individually or with cumulative statistical tests that searched for a faint signal present in multiple observations. The most promising burst observation based on the metrics was GRB 150323A, which is the focus of this paper.

The data are analyzed using a standard VERITAS analysis package with a selection of analysis parameters that is tuned to soft spectrum-sources, similar to Aliu et al. (2004), where the VERITAS follow-up observation of GRB 130427A is discussed. (GRB 130427A is a record-setting burst that reached the highest observed γ -ray fluence (Maselli et al. 2014).) The analysis we use here is similarly optimized for a source with an assumed photon index of approximately 3.5.

2. GRB 150323A

2.1. Observations of the Burst

On 2015 March 23, 02:49:14 UT, the *Swift*-BAT triggered on a burst with a J2000 position of (08^h32^m45^s.84, 45°26^m02^s.4) and an error radius of approximately 3 arcminutes (Amaral-Rogers et al. 2015). This error radius is both smaller than the VERITAS gamma-ray point-spread function ($\sim 0^{\circ}.1$) and the VERITAS field of view ($\sim 3^{\circ}.5$). This position was later refined with *Swift* X-ray telescope measurements to an accuracy of a few arcseconds (Goad et al. 2015). The optical afterglow was detected by the Low Resolution Imaging Spectrometer on the Keck I 10 m telescope. Several absorption and emission lines uniformly indicated the redshift of this burst to be $z = 0.593$ (Perley & Cenko 2015). A refined analysis by *Swift*-BAT (Markwardt et al. 2015) found the best-fit fluence in the 15–150 keV band to be 6.1×10^{-6} erg cm⁻². The best-fit photon index in the same spectral window was found to be 1.85.

VERITAS began observing the burst 270 s after the *Swift* trigger. The elevation of the source was 73° at that time, and slowly rising (until it reached its maximum elevation of 76°—an hour later—and began to decline). The observations lasted for

170 minutes. To produce the most sensitive result, we integrated only the first 40 minutes of the observation.²⁶ This was found to be ideal in the case of a burst that has a flux roughly decaying as $1/t$, as typically found by *Fermi*-LAT. The analysis yielded a result of 71 events in the on-source region, 563 events in the larger region used to estimate the background, and a relative normalization between the two regions, α , of 0.132, resulting in a significance of -0.36 , using Equation (17) of Li & Ma (1983).

We find the VERITAS differential upper limit (99% confidence level using the method described in Rolke et al. 2005) at 140 GeV is $3.7 \times 10^{-6} \text{ TeV}^{-1} \text{ m}^{-2} \text{ s}^{-1}$, and the integral upper limit from 140 GeV to 30 TeV is $1.6 \times 10^{-7} \text{ m}^{-2} \text{ s}^{-1}$. This upper limit assumes an intrinsic photon index of 2, and overlays extragalactic background light (EBL) absorption based on the model described in Finke et al. (2010); attenuation by the EBL increases rapidly above ~ 100 GeV and thus softens the observed spectrum of a distant source. Alternatively, the 99% confidence level upper limit can be given as 19.8 photons during the first 40 minutes of VERITAS observation.

From the differential upper limit for GRB 150323A at 140 GeV we can calculate a fluence per decade energy by assuming a photon index of 2, giving $6.4 \times 10^{-8} \text{ erg cm}^{-2}$. This corresponds to about 1% of the *Swift*-BAT detected prompt fluence.

VHE photons are known to interact with the EBL to produce electron-positron pairs, attenuating the intrinsic flux appreciably, and making sources difficult to detect from cosmological distances. The resulting gamma-ray attenuation for the VERITAS energy range becomes large at $z \gtrsim 1$, although this is somewhat EBL-model-dependent.²⁷ A redshift of 0.593 is among the lowest redshifts typically observed for a GRB (Coward et al. 2013).

The *Swift*-BAT light curve seen in Figure 1 places GRB 150323A into the ‘‘precursor’’ category, where most of the emission is produced tens to hundreds of seconds after a weak trigger event. These types of bursts can account for as few as 3% to as many as 20% of all bursts, depending on the criteria used to define them (Burlon et al. 2008). The light curve of GRB 150323A consists of one minor peak that triggered the observation, and a larger secondary peak about 135 s after the trigger. The VERITAS telescopes were on target 270 s after the BAT trigger at 02:53:44 UT, which corresponds to a 135 s delay compared to the main BAT peak. While the VERITAS observation is delayed relative to the prompt (BAT) emission, we stress that GeV observations by LAT consistently indicate a more temporally extended emission at higher photon energies (Ackermann et al. 2013). If this result extends to the VERITAS energy band, one would expect strong VHE emission, detectable by VERITAS at the time of observing. We note that GRB 150323A first entered the LAT field of view about an hour after the *Swift*-BAT trigger.

The VERITAS non-detection can be used to explore possible implications for GRB properties. We begin with an empirically driven calculation of the expected fluence in the VERITAS energy range, and conclude that the upper limit is strong and

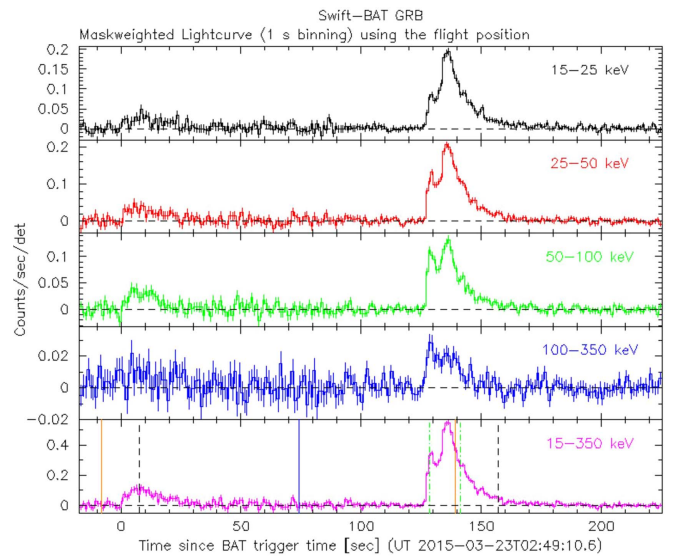


Figure 1. The *Swift*-BAT light curve for GRB 150323A, showing both the precursor and the main emission period. The different colored plots correspond to various energy bands observed by BAT, as indicated in each subplot. This image has been taken from the batgrbproduct analysis page: http://gc.gsfc.nasa.gov/notices_s/635887/BA/.

requires a more detailed theoretical analysis. Then, we discuss how the expected TeV emission depends on the blast wave energy and GRB environment, and how the measured upper limit constrains the prompt radiative efficiency and the density of the ambient medium.

2.2. Radiative Efficiency in the TeV Band

There are large variations among different bursts in the GeV fluence detected by LAT in comparison to the prompt fluence detected by GBM, and dimmer bursts also have light curves that decay more slowly (Lange & Pohl 2013). For brighter LAT-detected bursts, the energy emitted in the GeV band clusters around 10% of the GBM fluence (Ackermann et al. 2013). Assuming that comparable energy is emitted at higher frequencies, we calculated the expected fluence in the VERITAS band and divided it by the experimental upper limit. We have assumed that:

- (1) VHE emission begins suddenly and decays as $1/t$.²⁸
- (2) The fluence emitted in the VERITAS energy band is given by 10% of the prompt fluence detected by the BAT.²⁹
- (3) EBL absorption follows the model by Finke (Finke et al. 2010).³⁰

²⁸ We have the emission suddenly end after 1 day, which is consistent with the typical duration of a LAT observation.

²⁹ BAT and GBM cover nearby energy bands (Sakamoto et al. 2008), where in fact GBM covers a wider range of energies. In cases where the prompt emission peaks in the non-overlapping GBM band, this assumption is in fact conservative. This appears to be the case for GRB 150323A, given the hard 1.85 photon index observed by *Swift*-BAT (Markwardt et al. 2015).

³⁰ We use Finke et al. (2010), given that it is one of the more conservative (i.e., predicts more attenuation) among the recent EBL models. For example, at our threshold energy of 140 GeV ($z = 0.6$) Finke et al. (2010) give an attenuation factor of 0.47, whereas Gilmore et al.’s (2012) fiducial model and fixed model, Dominguez et al. (2011), and Franceschini et al. (2008) give factors of 0.42, 0.56, 0.55, and 0.57, respectively.

²⁶ The integration time is decided by a Monte Carlo simulation of a reasonable IACT background rate, and a $1/t$ signal at the threshold of detection. The simulation is designed to optimize the a priori expected significance for such a signal. One can find the results of an analysis of the full data set for GRB 150323A in Weiner (2015).

²⁷ As an example, according to the model described in Finke et al. (2010), at $z = 1$, about 85% of 140 GeV gamma-rays are absorbed.

Table 1
Ratio of the Model Fluence to the VERITAS Upper Limit under Different Assumptions

	VHE emission begins 1 s after trigger ^a	VHE emission begins 1 s after main peak (135 s)
Origin time at trigger	1.1	2.0
Origin time at 135 s	n/a	1.4

Note. The origin time corresponds to $t = 0$ in the $1/t$ time-decay. As an example, an origin time of 135 s could correspond to a burst that was independent of the triggering emission. The emission start time corresponds to the fluence budget of the tev radiation under assumption (2); see the text.

^a Consistent with LAT observations of prompt emission delay.

- (4) We approximate the VERITAS effective area as time-independent, while in reality it is very slightly changing during the observation.

Of these assumptions, we believe (2) is the most dependent on GRB environment and theory. Assumption (1) has been established by LAT data as a good approximation,³¹ (3) is in fact considered stringent in light of recent results (Abeysekara et al. 2015), and assumption number (4) is a very good approximation used for simplification purposes.

The resulting ratios are greater than 1 (see Table 1), indicating that the VHE emission must be weaker than expected by our extrapolation. This suggests a detailed discussion is needed, which we explore in the next section.

3. Theoretical Implications

The interaction between the relativistic GRB jet and the surrounding medium generates luminous high-energy emission. LAT-detected GeV emission is well-explained as radiation from the GRB blast wave loaded with electron-positron pairs (Beloborodov et al. 2014). The emission is naturally produced by inverse Compton (IC) scattering of prompt radiation by *thermal* pairs heated at the forward shock. The model provides good fits to the GeV data and was verified by the detection of the predicted optical counterparts with a special (model derived) light curve (Hascoët et al. 2015). In most cases, the theoretical spectra extend well above 100 GeV, where the emission can last from a few minutes up to a day. Below, we use this model to interpret the upper limit for GRB 150323A.

Recently, Vurm & Beloborodov (2017) conducted a systematic study of both simulated as well as observed GRBs exploding into different media; they concluded that the lack of detections by current Cherenkov instruments suggests that most of them explode into a dense medium, such as the stellar wind of the progenitor star. However, the case of GRB 150323A is somewhat special owing to its relatively weak X-ray afterglow (Melandri et al. 2015), resulting in fewer targets for IC emission. Consequently, one cannot conclusively rule out the ISM as the ambient medium in this burst.

3.1. Wind Medium

Given its relatively modest energy budget $\mathcal{E}_{\text{GRB}} \approx 10^{52}$ erg (Golenetskii et al. 2015), the jet of GRB 150323A expanding into the dense progenitor wind would have entered the self-similar deceleration regime by the time the VERITAS observation started. By this time, the dissipated luminosity at the forward shock is approximately $L_{\text{diss}} \sim \mathcal{E}_{\text{kin}}/(4t)$, where t is

the time in the cosmological rest frame of the burst. Particle-in-cell simulations of collisionless shocks suggest that a fraction $\varepsilon_e \sim 0.3$ of this energy is placed into heated thermal electrons (Sironi & Spitkovsky 2011). Unless the shock is strongly magnetized, the electrons radiate most of their energy via IC emission. The IC fluence received over a logarithmic time interval is

$$\mathcal{F}_{\text{IC}} \sim \frac{1+z}{4\pi d_L^2} t L_{\text{IC}} = 8.1 \times 10^{-7} \mathcal{E}_{\text{kin},52} \left(\frac{\varepsilon_e}{0.3} \right) \text{erg cm}^{-2}, \quad (1)$$

where $L_{\text{IC}} = \varepsilon_e L_{\text{diss}}$ and the normalization of the jet kinetic energy corresponds to 50% radiative efficiency ($\mathcal{E}_{\text{kin}} = \mathcal{E}_{\text{GRB}} = 10^{52}$ erg). We use the common notation that X_n corresponds to the quantity X divided by 10^n with suitable units so as to make the result dimensionless. Parameterizing the fraction of the IC energy that emerges in the VHE band as ε_{TeV} , the corresponding photon count at the detector is

$$\begin{aligned} \mathcal{N} &\sim A_{\text{eff}} \frac{\varepsilon_{\text{TeV}} \mathcal{F}_{\text{IC}}}{\bar{E}_{\text{ph}}} e^{-\tau_{\text{EBL}}} \\ &\approx 85 \mathcal{E}_{\text{kin},52} \left(\frac{A_{\text{eff}}}{5 \times 10^8 \text{cm}^2} \right) \left(\frac{\bar{E}_{\text{ph}}}{140 \text{GeV}} \right)^{-1} \left(\frac{\varepsilon_e}{0.3} \right) \left(\frac{\varepsilon_{\text{TeV}}}{0.1} \right), \end{aligned} \quad (2)$$

where $e^{-\tau_{\text{EBL}}} \approx 0.47$ accounts for attenuation by the EBL at 140 GeV (Finke et al. 2010).³²

The IC spectrum of the thermal electrons has approximately the same slope as the soft target radiation; the photons upscattered into the VHE band are typically from the X-ray domain. Given the observed X-ray photon index $\beta_X \approx 2.0$ (Melandri et al. 2015), the gamma-ray spectrum during the VERITAS observation is expected to be flat in terms of energy per logarithmic frequency interval. The spectrum cuts off at $E_{\text{max}} = \Gamma \gamma_{\text{th}} m_e c^2$, where γ_{th} is the average Lorentz factor of thermal electrons heated in the forward shock. Even if $E_{\text{max}} \gg 100$ GeV during the VERITAS observation, the observable window is limited: EBL absorption suppresses emission above $E \sim 300$ GeV, and the sensitivity of Cherenkov instruments declines below ~ 100 GeV. In this case $\varepsilon_{\text{TeV}} = 0.1$ is a reasonable estimate, and Equation (2) predicts about a hundred detectable counts, well above the upper limit of 20 from the 40-minute VERITAS observation. On the other hand, if $E_{\text{max}} \lesssim 100$ GeV throughout the observation, then effectively $\varepsilon_{\text{TeV}} = 0$ and no VHE emission is expected.³³ We consider it likely that this is the reason for the non-detection of GRB

³² See footnote 30.

³³ In our discussion we are neglecting the additional contribution from a possible non-thermal population of *accelerated* leptons. Their energy budget is expected to be significantly lower, but could also contribute to the VHE emission.

³¹ LAT results show that in the GeV band, afterglow fluence is comparable to prompt fluence, and decays approximately as $1/t$ (Ackermann et al. 2013).

150323A by VERITAS: the thermal IC emission cuts off below 100 GeV, while the IC component from non-thermal accelerated electrons is too weak to be detected.

Over most of the afterglow stage the maximal IC photon energy from thermal electrons is controlled by the Lorentz factor of the forward shock. However, during the first minute after the explosion, the prompt radiation ahead of the forward shock loads the ambient medium with a large number of pairs (Meszaros & Rees 1994; Thompson & Madau 2000; Beloborodov 2002); consequently, the average energy *per lepton* is low and E_{\max} is below the VHE band. The pair loading ends at (Thompson & Madau 2000; Beloborodov 2002)

$$R_{\text{load}} = 5.7 \times 10^{15} \mathcal{E}_{\text{GRB},52}^{1/2} \text{ cm}. \quad (3)$$

The turnover of the IC spectrum attains its maximal value at this radius:

$$\begin{aligned} E_{\max}(R_{\text{load}}) &\approx \Gamma \gamma_{\text{th}} m_e c^2 |_{R_{\text{load}}} \approx \Gamma^2 \mu_e \varepsilon_e m_p c^2 |_{R_{\text{load}}} \\ &= 440 \frac{\mathcal{E}_{\text{kin},52}}{A_{11} \mathcal{E}_{\text{GRB},52}^{1/2}} \left(\frac{\varepsilon_e}{0.3} \right) \text{ GeV}, \end{aligned} \quad (4)$$

where $\gamma_{\text{th}} = \Gamma \mu_e \varepsilon_e m_p / m_e$, A is the wind density parameter (a standard density Wolf–Rayet wind has $A \sim 3 \times 10^{11} \text{ g cm}^{-1}$), $\mu_e = 2$ is the mean molecular weight per proton in a Wolf–Rayet progenitor wind, and we have used $\Gamma = [\mathcal{E}_{\text{kin}} / (8\pi c^2 A R)]^{1/2}$ for the self-similarly decelerating blast wave. This occurs at observer time

$$t_{\text{load}} \approx \left. \frac{(1+z)R}{2c\Gamma^2} \right|_{R_{\text{load}}} = 190 \frac{A_{11}}{\mathcal{E}_{\text{kin},52}} \mathcal{E}_{\text{GRB},52} \text{ s}. \quad (5)$$

The VHE IC emission is suppressed at all times if $E_{\max}(R_{\text{load}}) < (1+z) \times 100 \text{ GeV}$, which yields a constraint

$$\frac{\mathcal{E}_{\text{kin},52}}{A_{11}} \lesssim 0.36 \mathcal{E}_{\text{GRB},52}^{1/2} \left(\frac{\varepsilon_e}{0.3} \right)^{-1} \text{ erg}. \quad (6)$$

This condition is marginally satisfied in a standard density Wolf–Rayet wind with $A \sim 3 \times 10^{11} \text{ g cm}^{-1}$ if the jet is at least moderately radiatively efficient in the prompt phase, i.e., $\mathcal{E}_{\text{kin}} \lesssim \mathcal{E}_{\text{GRB}} \approx 10^{52} \text{ erg}$.

In typical bursts, the pair-production opacity due to the X-ray afterglow photons suppresses the VHE emission at early times. However, for GRB 150323A it can be shown that attenuation by intrinsic $\gamma\gamma$ -absorption was at most marginal at $t \gtrsim 300 \text{ s}$ (after the steep early decline of the X-ray light curve), owing to its comparatively weak X-ray afterglow. It can also be shown that in a wind medium the weak X-ray afterglow nevertheless provides sufficient targets for marginally efficient IC cooling of the VHE emitting electrons.

3.2. ISM

In the low-density ISM the jet decelerates significantly later than in the wind medium, and $E_{\max} \gg 100 \text{ GeV}$ at R_{load} . The dissipation rate at the forward shock peaks at the deceleration radius

$$R_{\text{dec}} = \left(\frac{3\mathcal{E}_{\text{kin}}}{8\pi m_p c^2 n \Gamma_{\text{jet}}^2} \right)^{1/3} = 4.0 \times 10^{16} \frac{\mathcal{E}_{\text{kin},52}^{1/3}}{n^{1/3} \Gamma_{\text{jet},2}^{2/3}} \text{ cm}, \quad (7)$$

where Γ_{jet} is the initial jet Lorentz factor. The corresponding observer time for redshift $z = 0.6$ is $t_{\text{dec}} = 230 \mathcal{E}_{\text{kin},52}^{1/3} \Gamma_{\text{jet},2}^{-8/3} n^{-1/3} \text{ s}$.

Since $R_{\text{dec}} > R_{\text{load}}$, the VHE emission is also expected to peak near R_{dec} .

At $R > R_{\text{dec}}$ the shock-dissipated luminosity is $L_{\text{diss}} \sim 3\mathcal{E}_{\text{kin}}/(8t)$, i.e., comparable to that in the wind medium. However, owing to the larger characteristic R and Γ in the ISM, along with the weak X-ray afterglow of GRB 150323A, the shock-heated electrons are unable to cool/radiate efficiently. The ratio of expansion and IC cooling times for post-shock thermal electrons at t_{dec} is (Vurm & Beloborodov 2017)

$$\frac{t_{\text{dyn}}}{t_{\text{IC}}} = \frac{4\sigma_{\text{T}} u_{\text{X}} \gamma_{\text{th}}}{3m_e c} = 0.028 \frac{n^{1/3}}{\mathcal{E}_{\text{kin},52}^{1/3} \Gamma_{\text{jet},2}^{4/3}} L_{\text{X},46} \left(\frac{\varepsilon_e}{0.3} \right). \quad (8)$$

Here, L_{X} is X-ray afterglow luminosity that provides the targets for IC scattering and $u_{\text{X}} = L_{\text{X}} / (4\pi c R^2 \Gamma^2)$ is the comoving radiation energy density; in Equation (8) L_{X} is normalized to the observed value just after the steep decline that ends at $\sim 500 \text{ s}$.

In the slow-cooling regime the electrons radiate only a fraction $\sim t_{\text{dyn}}/t_{\text{IC}}$ of their energy before cooling adiabatically, which amounts to a few percent using our fiducial parameters. Including this factor, the count estimate (2) becomes consistent with a non-detection. Note, however, that the VERITAS observation started during the steep X-ray decay; the X-ray luminosity was above $10^{47} \text{ erg s}^{-1}$ for the first 50 s of observation. Although it suggests that VHE gamma-rays from this brief epoch could have been detectable, it does not constitute sufficient evidence to rule out the ISM as the environment of GRB 150323A.

4. Conclusions

We report the VERITAS observation of GRB 150323A, a promising candidate for the detection of VHE gamma-rays owing to its relative proximity ($z = 0.593$), high observing elevation, and the rapid response time of VERITAS, 270 s from the *Swift*/BAT trigger. No statistically significant signal was detected. We place a 99% confidence level differential upper limit on the 140 GeV fluence at $6.4 \times 10^{-8} \text{ erg cm}^{-2}$, which constitutes $\sim 1\%$ of the prompt fluence. For comparison, the average GeV fluence of LAT-detected GRBs is $\sim 10\%$ of the prompt (Ackermann et al. 2013) (unfortunately, no LAT observations are available for GRB 150323A). A naive extrapolation of the approximately flat spectra typically observed in the LAT band (in terms of νF_{ν}) would place a comparable amount of energy in the VHE band. The LAT emission usually peaks within the first $\sim 10 \text{ s}$, and decays as $t^{-\alpha}$, where $\alpha \sim 1$. Thus, even accounting for the additional delay, the deep VHE limit for GRB 150323A suggests that either (1) it had an intrinsically very weak high-energy afterglow (possibly hinted at by its weak X-ray afterglow), or (2) the GeV spectrum had a turnover below $\sim 100 \text{ GeV}$.

From a theoretical perspective, the energy dissipated by the relativistic blast wave of GRB 150323A would have been sufficient for a VERITAS detection if even $\sim 1\%$ of the dissipated energy was radiated in the VHE band, unless the prompt radiative efficiency was extremely high (i.e., almost no energy was left for the blast wave, $\mathcal{E}_{\text{kin}} \ll \mathcal{E}_{\text{GRB}}$). Using a “minimal” model where the high-energy emission is produced by shock-heated *thermal* electrons upscattering the (observed) X-ray afterglow radiation, we were able to place a constraint on the ratio of the blast wave kinetic energy and the ambient medium density. The high-energy turnover of the IC spectrum

remains below 100 GeV throughout the afterglow stage if GRB 150323A was a moderately radiatively efficient burst ($\mathcal{E}_{\text{kin}} \approx \mathcal{E}_{\text{GRB}}$) exploding into a standard Wolf–Rayet progenitor wind ($A \approx 3 \times 10^{11} \text{ g cm}^{-1}$). Alternatively, the blast wave would be dim in the VHE band at the time of the VERITAS observation if it exploded into a low-density ISM, due to inefficient cooling of the shock-heated electrons.

VERITAS is supported by grants from the U.S. Department of Energy Office of Science, the U.S. National Science Foundation and the Smithsonian Institution, and by NSERC in Canada. We acknowledge the excellent work of the technical support staff at the Fred Lawrence Whipple Observatory and at the collaborating institutions in the construction and operation of the instrument. The VERITAS Collaboration is grateful to Trevor Weekes for his seminal contributions and leadership in the field of VHE gamma-ray astrophysics, which made this study possible. I.V. acknowledges support from the Estonian Research Council grant PUT1112.

ORCID iDs

W. Benbow  <https://orcid.org/0000-0003-2098-170X>
 R. Bird  <https://orcid.org/0000-0002-4596-8563>
 W. Cui  <https://orcid.org/0000-0002-6324-5772>
 M. Errando  <https://orcid.org/0000-0002-1853-863X>
 Q. Feng  <https://orcid.org/0000-0001-6674-4238>
 J. P. Finley  <https://orcid.org/0000-0002-8925-1046>
 A. Furniss  <https://orcid.org/0000-0003-1614-1273>
 G. H. Gillanders  <https://orcid.org/0000-0001-8763-6252>
 D. Hanna  <https://orcid.org/0000-0002-8513-5603>
 C. A. Johnson  <https://orcid.org/0000-0002-0641-7320>
 P. Kaaret  <https://orcid.org/0000-0002-3638-0637>
 D. Kieda  <https://orcid.org/0000-0003-4785-0101>
 M. Krause  <https://orcid.org/0000-0001-7595-0914>
 M. J. Lang  <https://orcid.org/0000-0003-4641-4201>
 G. Maier  <https://orcid.org/0000-0001-9868-4700>
 R. Mukherjee  <https://orcid.org/0000-0002-3223-0754>
 J. S. Perkins  <https://orcid.org/0000-0001-9608-4023>
 M. Pohl  <https://orcid.org/0000-0001-7861-1707>
 A. Popkow  <https://orcid.org/0000-0002-3157-8839>
 E. Pueschel  <https://orcid.org/0000-0002-0529-1973>
 G. T. Richards  <https://orcid.org/0000-0002-1408-807X>
 K. Shahinyan  <https://orcid.org/0000-0001-5128-4160>

D. A. Williams  <https://orcid.org/0000-0003-2740-9714>
 Indrek Vurm  <https://orcid.org/0000-0003-1336-4746>

References

- Abdo, A. A., Allen, B. T., Berley, D., et al. 2007, *ApJ*, **666**, 361
 Abeysekara, A. U., Archambault, S., Archer, A., et al. 2015, *ApJL*, **815**, L22
 Acciari, V. A., Aliu, E., Arlen, T., et al. 2011, *ApJ*, **743**, 62
 Ackermann, M., Ajello, M., Asano, K., et al. 2013, *ApJS*, **209**, 11
 Ackermann, M., Ajello, M., Asano, K., et al. 2014, *Sci*, **343**, 42
 Aharonian, F., Akhperjanian, A. G., Barres de Almeida, U., et al. 2009, *A&A*, **495**, 505
 Albert, J., Aliu, E., Anderhub, H., et al. 2007, *ApJ*, **667**, 358
 Alfaro, R., Alvarez, C., Alvarez, J. D., et al. 2017, *ApJ*, **843**, 88
 Aliu, E., Aune, T., Barnacka, A., et al. 2004, *ApJL*, **795**, L3
 Amaral-Rogers, A., Barthelmy, S. D., Marshall, F. E., et al. 2015, *GCN Circ.*, **17611**
 Atkins, R., Benbow, W., Berley, D., et al. 2000, *ApJL*, **533**, L119
 Barthelmy, S. 2008, *AN*, **329**, 340
 Beloborodov, A. M. 2002, *ApJ*, **565**, 808
 Beloborodov, A. M., Hascoët, R., & Vurm, I. 2014, *ApJ*, **788**, 36
 Burlon, D., Ghirlanda, G., Ghisellini, G., et al. 2008, *ApJL*, **685**, L19
 Coward, D. M., Howell, E. J., Branchesi, M., et al. 2013, *MNRAS*, **432**, 2141
 Dominguez, A., Primack, J. R., Rosario, D. J., et al. 2011, *MNRAS*, **410**, 2556
 Finke, J. D., Razzaque, S., & Dermer, C. D. 2010, *ApJ*, **712**, 238
 Franceschini, A., Rodighiero, G., Vaccari, M., et al. 2008, *A&A*, **487**, 837
 Gilmore, R. C., Somerville, R. S., Primack, J. R., et al. 2012, *MNRAS*, **422**, 3189
 Goad, M. R., Osborne, J. P., Beardmore, A. P., et al. 2015, *GCN Circ.*, **17615**
 Golenetskii, S., Aptekar, R., Frederiks, D., et al. 2015, *GCN Circ.*, **17640**
 Hascoët, R., Vurm, I., & Beloborodov, A. M. 2015, *ApJ*, **813**, 63
 Holder, J., Acciari, V. A., Aliu, E., et al. 2009, in *AIP Conf. Proc.* 1085, HIGH ENERGY GAMMA-RAY ASTRONOMY: Proceedings of the 4th International Meeting on High Energy Gamma-Ray Astronomy (Melville, NY: AIP), **657**
 Lange, J., & Pohl, M. 2013, *A&A*, **551**, 89
 Li, T.-P., & Ma, Y.-Q. 1983, *ApJ*, **272**, 317
 Markwardt, C. B., Amaral-Rogers, A., Barthelmy, S. D., et al. 2015, *GCN Circ.*, **17628**
 Maselli, A., Melandri, A., Nava, L., et al. 2014, *Sci*, **343**, 48
 Melandri, A., D’Avanzo, P., & D’Elia, V. 2015, *GCN Circ.*, **17618**
 Meszaros, P., & Rees, M. J. 1994, *MNRAS*, **269**, L41
 Park, N. 2005, *Proc. ICRC*, arXiv:1508.07070
 Perley, D. A., & Cenko, S. B. 2015, *GCN Circ.*, **17616**
 Rolke, W. A., López, A. M., & Conrad, J. 2005, *NIMPA*, **551**, 493
 Sakamoto, T., Barthelmy, S. D., Barbier, L., et al. 2008, *ApJ*, **175**, 179
 Sironi, L., & Spitkovsky, A. 2011, *ApJ*, **726**, 75
 Thompson, C., & Madau, P. 2000, *ApJ*, **538**, 105
 Vurm, I., & Beloborodov, A. M. 2017, *ApJ*, **846**, 152
 Weiner, O. M. 2015, *Proc. ICRC*, arXiv:1509.01290